Effect of Charge Transfer on the Structure of Stage–1 Alkali Metal Graphite Intercalation Compounds: A First Principles Study

G. Overney, W. Zhong, and D. Tománek

Department of Physics and Astronomy and

Center for Fundamental Materials Research

Michigan State University, East Lansing, Michigan 48824–1116

(Received)

Abstract

Using *ab initio* Density Functional Theory, we determine changes of the equilibrium structure of graphite due to charge transfer between the alkali intercalant atoms and the host layers. From our self-consistent calculations, we show for stage–1 Li and K graphite intercalation compounds that there is a deviation from a universal relationship between charge transfer and the C–C bond length. We find the transferred charge, stemming from intercalant atoms, to be very localized at the carbon sites adjacent to the intercalants. Our results also include the activation energy E_a for the diffusion of Li atoms in the galleries of LiC_6.

62.20.Dc, 61.50.Lt, 66.30.Dn

1

During the past three years, several attempts have been undertaken to obtain space-resolved information on structural and electronic properties of graphite intercalation compounds (GIC's) using Scanning Tunneling Microscopy (STM) [1,2] and Atomic Force Microscopy (AFM) [3]. Past theoretical work has concentrated on the electronic structure of GIC's, specifically on the effect of intercalants on the electronic states of the system. While the lattice expansion due to donor intercalants is generally well established [4], relatively little is known about the dependency of these structural changes on the intercalant species and their concentration. Substantial controversy still remains regarding the question, whether the donor charge is localized or rather delocalized, the latter behavior being suggested by the success of the rigid band model for the band structure of GIC's. Finally, very little is known about the diffusion kinetics of intercalants during the formation of GIC's.

In this paper, we address these questions in stage–1 alkali–metal GIC's LiC_2, LiC_6, LiC_8, KC_6, and KC_8, and focus our interest on the relationship between charge transfer and structural changes. First we investigate changes of the C–C in–plane bond length d_{C-C} due to charge transfer which occur in relation to the nearest neighbor distance in pure graphite in various donor GIC's. X–ray diffraction experiments of Nixon et al. [5] indicated an in–layer lattice expansion which increases from stage–1 to stage–6 potassium GIC's. Second, we investigate the charge distribution in donor compounds. We focus on stage–1 Li GIC's and show that the charge transferred from the intercalant to the graphite layers is spatially very localized. Third, we calculate the activation energy E_a for the diffusion of Li atoms in the host galleries of LiC_6.

We intend to address these problems from first principles, without any adjustable parameters. We use the Local Density Approximation (LDA) to calculate the total energy and the corresponding charge distribution [6,7]. We replace the ionic potentials by ab initio pseudopotentials, generated using the scheme of Hamann, Schlüter, and Chiang [8]. Core corrections are considered for the alkali atoms. The exchange–correlation energy is parametrized according to Hedin and Lundqvist [9]. The Wannier functions are expanded in a linear combination of local Gaussian–type orbitals. These orbitals are centered on

atomic sites and, in selected cases, the basis is extended by floating orbitals on interstitial sites. At each atomic site (intercalant and carbon atom), we consider s, p_x, p_y, and p_z orbitals with three radial Gaussian decays each, i.e. twelve independent basis functions. For carbon, the decay constants which yield the minimum total energy of graphite are $\alpha(C) = 0.24$, 0.797, and 2.65 [10,11]. For Li and K, $\alpha(Li) = 0.10$, 0.17, 0.387 and $\alpha(K) = 0.10$, 0.22, 0.50 are obtained by minimizing the total energy of the bulk metal.

It is well known that the LDA strongly underestimates Van der Waals interactions which, together with weak interactions due to interlayer hybridization, establish the interlayer interaction in graphite. The fact that LDA correctly predicts the equilibrium structure and elastic properties of pristine graphite [12] establishes the importance of weak chemical interlayer interactions in the cohesion of graphite. While LDA describes correctly pristine graphite, it is expected to give even more reliable results for intercalation systems where cohesion is dominated by strong ionic and chemical bonds.

Therefore, we use this approach to determine the equilibrium structures and the total energies for KC_x, LiC_x ($x = 6$ and 8) and the hypothetical system LiC_2 which has not been observed [13]. We use an energy cutoff of typically $49 - 56$ Ry in the Fourier expansion of the charge density in order to ensure a complete convergence of the LDA spectrum and the total energies. Our calculations show that in the case of the LiC_x systems, complete convergence can only be achieved with a relatively high energy cutoff of ≈ 56 Ry. For pristine graphite (highly oriented pyrolytic graphite, HOPG) and the KC_x compounds, an energy cutoff of 49 Ry is sufficient. The LDA charge density and potentials are obtained by sampling the irreducible part of the Brillouin zone by a mesh of 24 special $\vec{k}$ points [14] for KC_8 and LiC_8; 21 $\vec{k}$ points are used for KC_6, LiC_6, LiC_2, and pristine graphite.

The geometries of MC_x ($x = 2$, 6, and 8) are displayed in Fig. 1 [15]. In Fig. 2, we show the total energy change per unit cell as a function of the interlayer separation c and the intralayer bond length d_{C-C}. Figs. 2(a) and 2(b) show $E_{tot}(LiC_6)$, as a function of d_{C-C} and c. The corresponding results for KC_8 are given in Figs. 2(c) and 2(d). For the small displacements which have been considered, the system response has only negligible

3

anharmonic contributions, and the LDA values can be fitted with a second order polynomial function. In Table I, we summarized all calculated equilibrium lattice parameters d_{C-C} and c together with the experimental data for the structures investigated in this work. We find our LDA results to be in generally good agreement with the experiment, with the exception of the interlayer separation c for KC_8 which shows a large difference between the observed and calculated value (c_{exp} = 5.35 Å and c_{LDA} = 5.70 Å). The likely reason for this difference is the constraint in our LDA calculations that the graphite layers not buckle in the GIC's. This assumption is reasonable for large intercalant concentrations and the assumed AA stacking of both the intercalants and the graphite layers. In the case of LiC_6, which has this structure [15], this procedure leads to the experimentally observed values for d_{C-C} and c. In the more dilute KC_8 compound, the system can gain structural energy by horizontally shifting the intercalant layers by a fraction of a lattice constant and buckling the graphite layers, as indicated schematically in Fig. 1(b). This relaxation energy stabilizes the $A_\alpha A_\beta A_\gamma A_\delta$ structure of KC_8 [15] and reduces the *average* interlayer spacing $< c >$ with respect to a value expected from rigid graphite layers. The buckling of the relatively rigid graphite layers is moderate and does not result in significant changes of d_{C-C}.

In the case of LiC_6, we considered two different sites for the lithium atoms in the $\sqrt{3} \times \sqrt{3}$ superstructure, namely the hollow site (atop and below the center of a hexagon) and the bridge site (atop and below the center of a C–C bond). The latter site has been shown by DiVincenzo *et al.* to be a saddle point of the total energy surface [16]. It is most likely that the diffusion of Li atoms between adjacent hollow sites proceeds via the bridge site and not the "on–top" site, since the Coulomb repulsion makes the latter site energetically less favorable. Consequently, we define the activation energy E_a for the diffusion of a Li atom in a gallery as

$$E_a = E_{tot}(\text{bridge site}) - E_{tot}(\text{hollow site}). \tag{1}$$

To obtain E_{tot}(hollow site), we minimized the total energy of the system with respect to the nearest neighbor bond length d_{C-C} and the interlayer spacing c. The calculated value of

the energy associated with the diffusion of a Li atom along the galleries is $E_a = 0.39$ eV. This value is much smaller than the previously calculated value $E_a = 1.30$ eV of DiVincenzo et al. [16]. The main reason for the discrepancy is the simplification of the valence charge density ρ_ν underlying the calculation of Ref. [16], which is based on an isolated graphite monolayer. Our LDA calculation does not make this simplifying assumption, as it treats the LiC$_6$ system fully self–consistently. We find our calculated activation energy to be in reasonable agreement with the value $E_a = 0.66$ eV of Freilander et al. [17], based on β–NMR experiments. The in–plane diffusion constant D is related to E_a by [16]

$$D \approx 3 \times d_{C-C}^2 \nu_0 e^{-E_a/kT}, \tag{2}$$

where ν_0 is an in–plane alkali vibrational frequency and d_{C-C} the nearest neighbor C–C distance ($d_{C-C} = 1.416$ Å). This intercalant hopping model has been known to provide a good description of the diffusion of "heavy" alkali atoms (Rb and Cs) along the galleries. The observed diffusion of Li atoms in galleries is substantially larger than suggested by the simple hopping model of Eq. (2), if the experimental value $E_a = 0.66$ eV of Ref. [17] were used. While the applicability of this diffusion model to Li in graphite may still be questioned, we note that our calculated lower activation barrier $E_a = 0.39$ eV, used in Eq. (2), would suggest much higher diffusion of Li, which would be in much better agreement with experimental data.

Our calculated value for the equilibrium C–C bond length in AA–stacked graphite is $d_{C-C} = 1.4157$ Å, which compares well with the experimental value $d_{C-C} = 1.421$ Å [5]. In the following, we will relate all changes in d_{C-C} (denoted as Δd_{C-C}) to our LDA value for graphite (1.4157 Å).

We found the equilibrium structure of KC$_8$ to be characterized by $d_{C-C} = 1.4305$ Å ($\Delta d_{C-C} = 0.0148$ Å) and $c = 5.70$ Å. As mentioned above, this is in resonable agreement with the experimental result $d_{C-C} = 1.432$ Å [18]. The corresponding values for KC$_6$ are $d_{C-C} = 1.4312$ Å ($\Delta d_{C-C} = 0.0155$ Å) and $c = 5.90$ Å.

In order to better understand the effect of intercalants on the graphite lattice, we have

extended our calculations to LiC_2 and LiC_8. The calculated equilibrium values for the lattice parameters d_{C-C} and c are listed in Table I. The changes of the C–C bond length for different intercalant species and concentrations are also shown in Fig. 3. The results indicate that for alkali intercalation compounds MC_x, Δd_{C-C} is nearly proportional to the intercalant concentration $1/x$, as suggested earlier by Chan *et al.* [19]. The calculation of Ref. [19] addressed systematic changes of the C–C bond length for generic donor and acceptor compounds at different intercalant concentrations. The intercalants have been modeled by ions of charge Z, located midway between graphite layers in the filled galleries for a given intercalation stage. While the agreement between this model and experimental data is quite good, especially for the higher stages ($n \geq 2$), we find deviation from the universal behavior in the more concentrated systems.

The lattice dilation in donor compounds has two main origins, both of which can be understood using the rigid band model underlying the calculation of Ref. [19]. The charge transferred from the donor sites gets predominantly accommodated in the lone $2p_z$ orbitals of the graphite layers, which are empty and lie energetically at the Fermi surface in pristine graphite [20]. The slightly antibonding nature of these orbitals with respect to second-neighbor intralayer π bonds causes a lattice expansion upon charge transfer [20]. A weaker, secondary effect observed upon donor intercalation is a depletion of the strongly bonding intralayer σ bonds which augments the lattice expansion. This lattice dilation mechanism agrees with that proposed originally by Pietronero and Strässler [21].

Our results for Δd_{C-C} in stage–1 GIC's, shown in Fig. 3, indicate deviations from a universal behavior for generic alkali intercalants. Specifically, we note that d_{C-C} depends very weakly on the intercalant concentration in K–based GIC's, while the data for Li-based GIC's nearly follow the universal curve. This behavior can be explained in terms of the hybridization between the donor and the graphite orbitals and an inhomogeneous distributions of the donor charge across the graphite layers, both of which are beyond the scope of the simple rigid-band model.

In order to understand the spatial distribution of the charge transferred between the

intercalants and the graphite matrix, we display the difference charge density $\Delta\rho$ in Li-based GIC's at two different Li concentrations in Fig. 4 [22]. Both Figs. 4(a) and 4(b) show clearly a charge transfer towards the $C2p_z$ orbitals, the constituents of the antibonding π system, and a charge depletion in the bonding σ system. In LiC_6, addressed in Fig. 4(a), all carbon atoms are equivalent and receive the same transferred charge ΔQ. The degree of localization of the transferred charge in the graphite layers near intercalant sites can be studied best in the more dilute LiC_8 system which has two inequivalent C atoms per unit cell. The calculated difference charge density for LiC_8 is shown in Fig. 4(b). In order to estimate the total charge on carbon and intercalant atoms, without resorting to a projection onto a localized basis, we first divided the Wigner–Seitz cell of the original graphite matrix into halves by a plane located midway between the carbon and intercalant layers [see Fig. 4(b)]. The half containing the carbon layers has been further subdivided into equal parts, which were subsequently associated with the two carbon atoms of the graphite basis. The charge ΔQ_i transferred to the two inequivalent carbon sites has been estimated by integrating $\Delta\rho$ over the respective box volume. We found a large ratio $\Delta Q_1/\Delta Q_2 \approx 5$, indicating a strong spatial localization of the donor charge on the carbon atoms adjacent to the intercalants. This charge inhomogeneity causes a large difference in the crystal potential at the two carbon atoms in the unit cell, which is expected to substantially modify the electronic states of the underlying graphite lattice and to cause a deviation from universal lattice expansion.

More important than the above mentioned differences in charge transfer is the hybridization between intercalant and graphite orbitals, which is explicitly neglected in the rigid band model underlying the universal curve shown in Fig. 3. In general, we expect a stronger intercalant–carbon hybridization for the more diffuse $K4s$ orbitals than the tightly bound $Li2s$ orbitals. These effects can be seen in the electronic density of states (DOS), which we show in Fig. 5 for stable Li– and K– based GIC's. A comparison between the pristine graphite and the LiC_6 results [see Figs. 5(a) and (b)] suggests that the respective densities of states are very similar, the main difference being the position of the Fermi level [23]. This provides *a posteriori* support for the applicability of the rigid band model in the Li interca-

lation compounds, as discussed above and in Ref. [24], and explains why the deviation from the universal curve in Fig. 3 should be small in Li systems.

The situation is significantly different for KC_8, as shown in Fig. 5(c). An inspection of the density of states close to the Fermi level indicates strong differences with respect to pristine graphite. Caused mainly by a strong intercalant–graphite hybridization, we observe a gap opening at the Fermi level, which strongly modifies the density of states of the underlying graphite. We expect a departure from the rigid band behavior, and consequently a strong deviation from a universal behavior, as confirmed by our results in Fig. 3.

We should note that the charge localization near the intercalant sites, which we discussed above, is also expected to cause a spatial modulation of the elastic response of the graphite layers. This is a consequence of the effect of charge transfer on the intra–layer bonding, which among others modifies the frequencies of the in–plane E_{2g_2} and out–of–plane A_{2u} modes of graphite [12,25]. This mode softening is a consequence of local modifications of the elastic constants — such as the flexural rigidity — near intercalant sites. A spatial variation of the flexural rigidity near isolated donor impurities in the topmost gallery of graphite should be observable in Atomic Force Microscopy, as postulated in Ref. [26].

In conclusion, we have calculated structural and electronic properties of Li– and K–based GIC's using an *ab initio* LDA formalism. We have shown that the charge transferred between the intercalant sites and the graphite matrix is strongly localized on carbon atoms adjacent to the intercalants, providing support for a strong spatial variation of the elastic behavior in GIC's. The kinetics of intercalants in GIC's has been addressed by calculating the activation barrier E_a for the diffusion of Li atoms in the galleries of LiC_6. Our value $E_a = 0.39$ eV is in good agreement with β–NMR experiments and the observed diffusion constant. Finally, we have determined the equilibrium structures of LiC_x and KC_x compounds by optimizing the C–C bond length d_{C-C} and the interlayer spacing c for different intercalant concentrations x. We find the increase in d_{C-C} to be roughly proportional to the alkali intercalant concentration. This is expected based on a rigid band model which predicts a species–independent lattice expansion in all alkali–based GIC's. We find sub-

stantial deviations form this behavior especially in stage–1 K–based GIC's. The origin of this nonuniversality can be traced back to a spatial localization of the transferred charge at carbon sites adjacent to intercalants, and significant hybridization between the intercalant atoms and the graphite layers.

REFERENCES

[1] D. Anselmetti, R. Wiesendanger, and H.–J. Güntherodt, Phys. Rev. B **39**, 11135 (1989).

[2] D. Anselmetti, V. Geiser, G. Overney, R. Wiesendanger, and H.-J. Güntherodt, Phys. Rev. B **42**, 1848 (1990).

[3] E. Meyer and R. M. Overney (private communication).

[4] D. P. DiVincenzo and S. Rabii, Phys. Rev. B **25**, 4110 (1982); M. Y. Chou, M. L. Cohen, and S. G. Louie, Phys. Rev. B **33**, 6619 (1986); S. Rabii, J. Chomilier, and G. Loupias, Phys. Rev. B **40**, 10105 (1989), and references therein.

[5] D. E. Nixon and G. S. Parry, J. Phys. C **2**, 1732 (1969).

[6] P. Hohenberg and W. Kohn, Phys. Rev. **136**, B864 (1964).

[7] W. Kohn and L.J. Sham, Phys. Rev. **140**, A1133 (1965).

[8] D.R. Hamann, M. Schlüter, and C. Chiang, Phys. Rev. Lett. **43**, 1494 (1979).

[9] L. Hedin and B.J. Lundqvist, J. Phys. C **4**, 2064 (1971).

[10] D. Tománek and S.G. Louie, Phys. Rev. B **37**, 8327 (1988).

[11] S. Fahy, Steven G. Louie, and Marvin L. Cohen, Phys. Rev. B **34**, 1191 (1986).

[12] G. Overney, D. Tománek, W. Zhong, Z. Sun, H. Miyazaki, S. D. Mahanti, and H.-J. Güntherodt, J. Phys.: Cond. Mat. **4**, 4233 (1992).

[13] The stoichiometry with the largest metal concentration is MC_6, which has been recently observed in STM measurements of K–based GIC's (H.P. Lang, private communication).

[14] D.J. Chadi and M.L. Cohen, Phys. Rev. B **8**, 5747 (1973).

[15] In all self–consistent LDA calculations of stage–1 compounds, we assume AA–stacking for both the graphite *and* the intercalant layers. In LiC_6, this $A_\alpha A_\alpha A_\alpha A_\alpha$ stacking has been experimentally confirmed. In the KC_8 structure, on the other hand, a more

complex $A_\alpha A_\beta A_\gamma A_\delta$ stacking has been proposed. In this notation, the graphite layers are referred to by Roman and the intercalant atoms by Greek letters. Since the shift in the interlayer separation is mainly given by the structural arrangement of the intercalants within one gallery, our simplifying assumption does not affect the quantitative results for the intralayer bond length d_{C-C} and the interlayer spacing.

[16] D. P. DiVincenzo and E. J. Mele, Phys. Rev. Lett. **53**, 52 (1984).

[17] P. Freilander, P. Heitjans, H. Ackermann, B. Bader, G. Kiese, A. Schirmer, H.–J. Stöckmann, C. Van der Marel, A. Magerl, and H. Zabel, Z. Phys. Chem. NF **151**, 93 (1987).

[18] P. La Grange, D. Guérard, and A. Hérold, Ann. Chim. **3**, 143 (1978).

[19] C. T. Chan, W. A. Kamitakahara, K. M. Ho, and P. C. Eklund, Phys. Rev. Lett. **58**, 1528 (1987).

[20] M. Kertesz, F. Vonderviszt, and R. Hoffman, Mat. Res. Soc. Symp. Proc. **20**, 141 (1983).

[21] L. Pietronero and S. Strässler, Phys. Rev. Lett. **47**, 593 (1981).

[22] The difference charge density $\Delta\rho$ of GIC's is given with respect to pristine graphite, assuming the same positions for the carbon atoms.

[23] Deviations from a rigid band behavior in LiC_6, which are seen in Fig. 5(b) especially above E_F, have been addressed by R. V. Kasowski, Phys. Rev. B **25**, 4189 (1982), and associated with a distortion of the π states of graphite. This modification of the empty states has no effect on the structural properties of LiC_6.

[24] N. A. W. Holzwarth, S. G. Louie, and S. Rabii, Phys. Rev. B **28**, 1013 (1983).

[25] C. T. Chan, K. M. Ho, and W. A. Kamitakahara, Phys. Rev. B **36**, 3499 (1987).

[26] D. Tománek, G. Overney, H. Miyazaki, S. D. Mahanti, and H.–J. Güntherodt, Phys. Rev. Lett. **63**, 876 (1989) and ibid. **63**, 1896(E) (1989).

[27] M. S. Dresselhaus and G. Dresselhaus, Advances in Physics **30**, 139 (1981).

[28] D. Guérard and A. Hérold, Carbon **13**, 337 (1975).

TABLES

TABLE I. Calculated and observed lattice parameters d_{C-C} and c for pristine graphite and stage–1 alkali–metal based graphite intercalation compounds.

	d_{C-C} (LDA)	d_{C-C} (expt.)	c (LDA)	c (expt.)
Graphite [a]	1.4157 Å	1.421 Å[b]	3.36 Å	3.35 Å[c]
LiC$_2$	1.4837 Å	–	3.45 Å	–
LiC$_6$	1.4338 Å	1.435 Å[d]	3.65 Å	3.70 Å[d]
LiC$_8$	1.4289 Å	–	3.66 Å	–
KC$_6$	1.4312 Å	–	5.90 Å	–
KC$_8$	1.4305 Å	1.432 Å[b]	5.70 Å	5.35 Å[e]

[a]AA stacking.

[b]Reference [5].

[c]Reference [27].

[d]Reference [28].

[e]Reference [18].

FIGURES

FIG. 1. Schematic view of the atomic arrangement in graphite intercalation compounds (GIC's). (a) Side view of the gallery. Solid lines indicate the graphite layers. Carbon and intercalant atoms are given by small and large solid circles, respectively. (b) Side view of a gallery, illustrating how graphite layer buckling can affect the stacking of intercalant layers. (c) Top view of MC_2 (1 × 1), MC_6 ($\sqrt{3} \times \sqrt{3}$), and MC_8 (2 × 2) (the intercalant atoms are given by the black solid circles).

FIG. 2. Total energy per unit cell as a function of the nearest neighbor distance d_{C-C} and the interlayer spacing in LiC_6 ((a), (b)) and KC_8 ((c), (d)). The solid lines are second order polynomial fits to the LDA data (given by •).

FIG. 3. The change of the C–C bond length Δd_{C-C} with respect to graphite in MC_x systems as function of $1/x$. The solid line denotes the results of Chan *et al.* [19]. The LDA results for KC_x are given by * and those for LiC_6 by ◇.
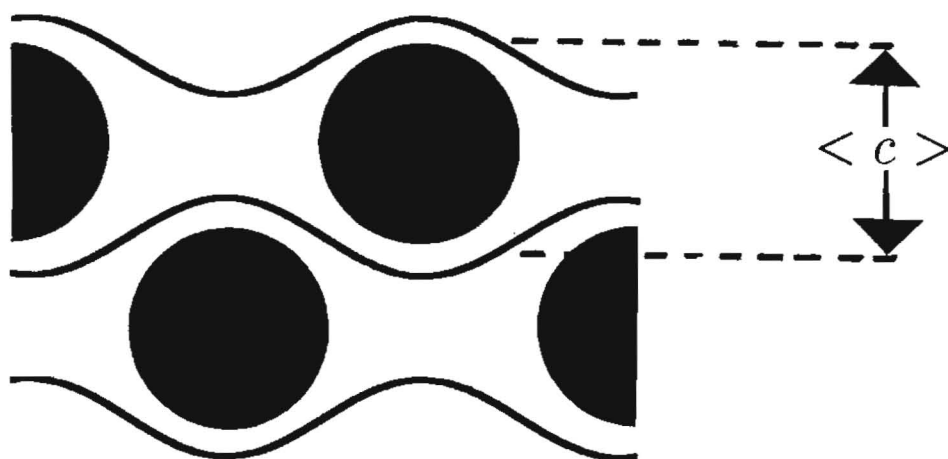
FIG. 4. Contour plot of the difference charge density $\Delta\rho$ for (a) LiC_6 and (b) LiC_8, in a plane perpendicular to the graphite layers. $\Delta\rho$ is given with respect to pristine graphite, assuming the same positions for the carbon atoms. Excess charge is indicated by solid lines, charge deficit by dashed lines. A linear contour increment of 10^{-3} el./(a.u.)^3 is used. The highest contour value is 15.46×10^{-3} el./(a.u.)^3 in (a) and 11.08×10^{-3} el./(a.u.)^3 in (b). Positions of the carbon atoms are marked by * and those of Li atoms by ×.

FIG. 5. Electronic density of states (DOS) for (a) AA–stacked graphite, (b) LiC_6, and (c) KC_8. Energies are referenced to the Fermi level E_F, marked by the dashed line.
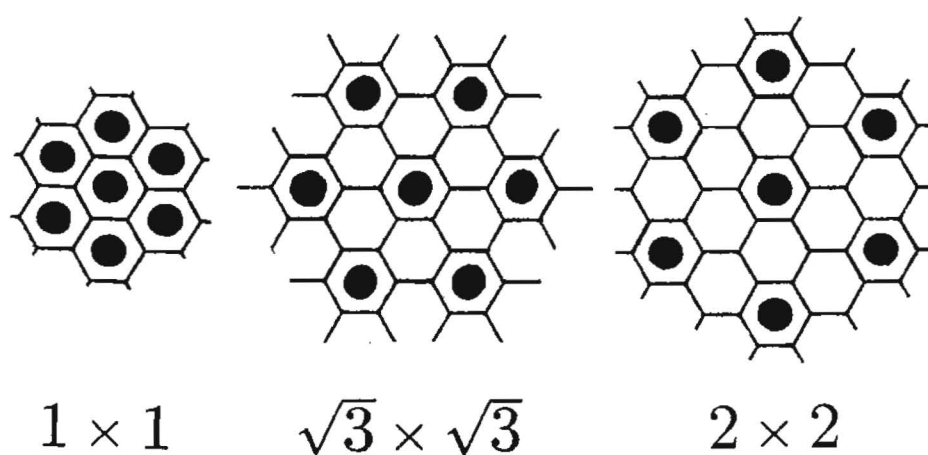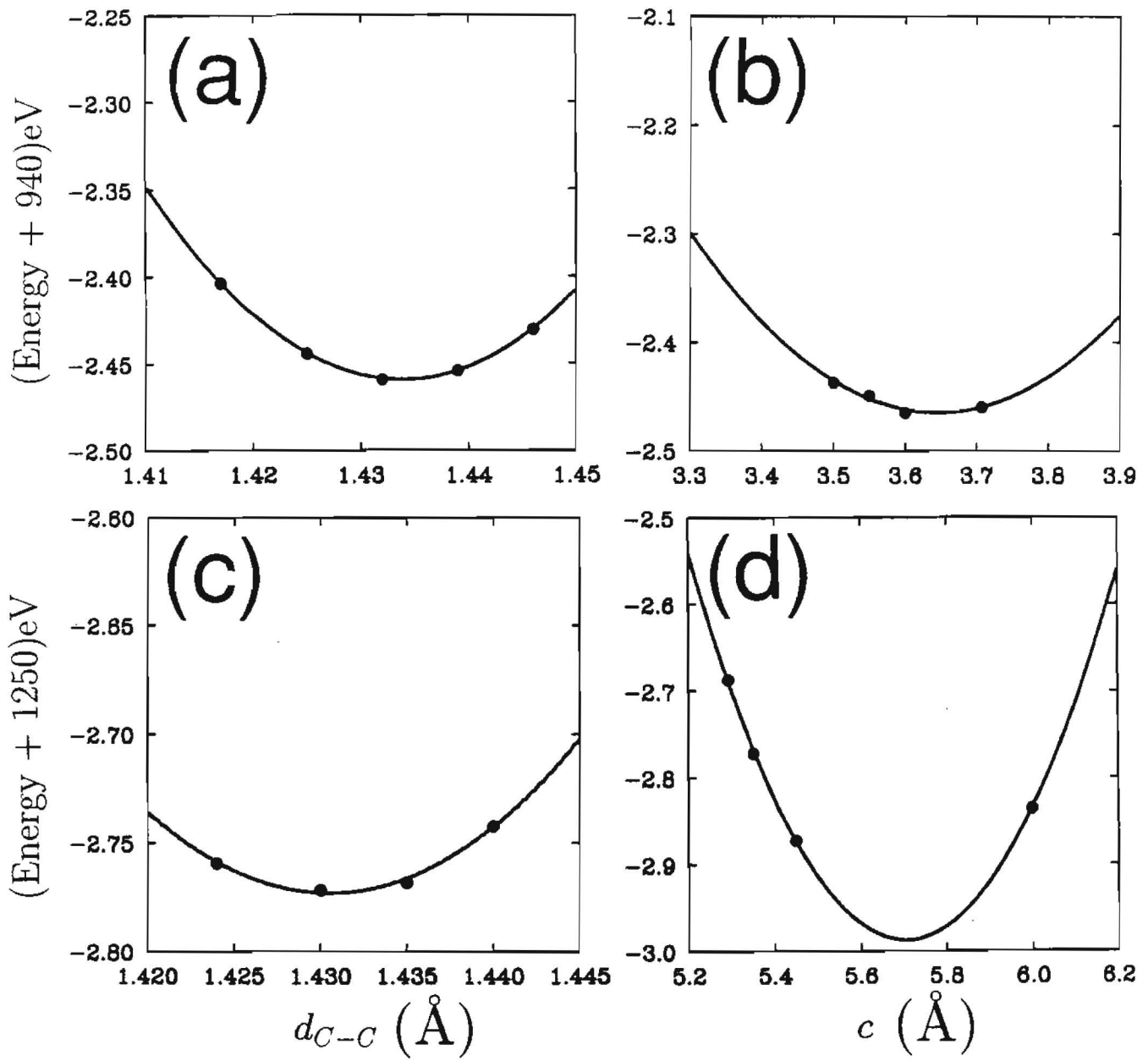
14

(a)

c

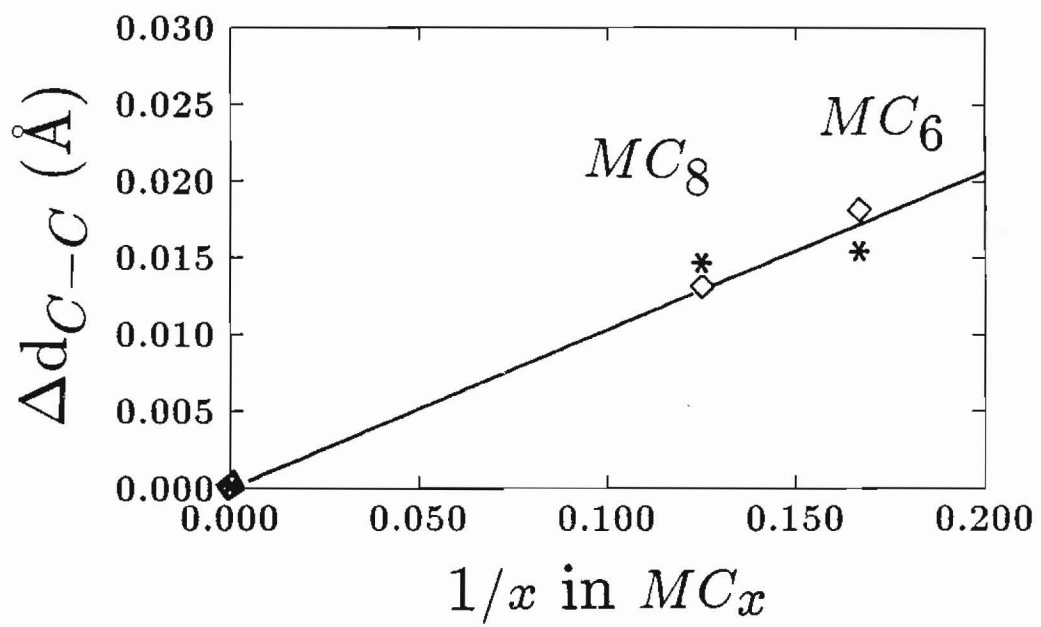$d_{\text{C–C}}$

(b)

$\langle c \rangle$

(c)

1×1 $\sqrt{3} \times \sqrt{3}$ 2×2

Fig. 1

Fig. 2

Fig. 3

(a)

- - C

- - Li

- - C

(b)

1 2

- - C

- - Li

- - C

Fig. 4

Fig. 5